Hydrogen Bonding Interactions of Pyridine$^{\bullet+}$ with Water: Stepwise Solvation of Distonic Cations

Yehia Ibrahim, Ridha Mabrouki, Michael Meot-Ner,* and M. Samy El-Shall*

Department of Chemistry, Virginia Commonwealth University Richmond, Virginia 23284-2006

Received: November 8, 2006

The solvation energies of the pyridine$^{\bullet+}$ radical cation by 1−4 H_2O molecules were determined by equilibrium measurements in a drift cell. The binding energies of the pyridine$^{\bullet+}(H_2O)_n$ clusters are similar to the binding energies of protonated pyridine−water clusters, $(C_5H_5NH^+)(H_2O)_n$, which involve $NH^+\cdot\cdot OH_2$ bonds and different from those of the solvated benzene radical cation−water clusters, $C_6H_6^{\bullet+}(H_2O)_n$, which involve $CH^{\delta+}\cdot\cdot OH_2$ bonds. These relations indicate that the observed pyridine$^{\bullet+}$ ions have the distonic $^{\bullet}C_5H_4NH^+$ structures that can form $NH^+\cdot\cdot OH_2$ bonds. The observed thermochemistry and ab initio calculations show that these bonds are not affected significantly by an unpaired electron at another site of the ion. Similar observations also identify the 2-fluoropyridine$^{\bullet+}$ distonic ion. The distonic structure is also consistent with the reactivity of pyridine$^{\bullet+}$ in H atom transfer, intra-cluster proton transfer and deprotonation reactions. The results present the first measured stepwise solvation energies of distonic ions, and demonstrate that cluster thermochemistry can identify distonic structures.

I. Introduction

Distonic ions are radical ions that contain a charge center, and a separate radical site. For protonated molecules, distonic isomers are formally related to conventional cations by an H atom shift $H-CRX^{\bullet+} \rightarrow {}^{\bullet}CRX-H^+$ to a heteroatom.

The distonic ions can be reaction intermediates,[1,2] or stable isomers.[3−6] Distonic ions can be characterized by their collisional dissociation (CID) and by neutralization−reionization,[7−16] and by distinctive ion−molecule reactions[4,16−21] Relevant to the present study, N-protonated distonic structures were reported in ionized pyridine itself[7,8] and in ionized pyridine derivatives.[22−28] The reactions of distonic pyridine with several neutrals were studied under low-pressure energetic CID conditions. In these systems the distonic ion extracts an O atom from water to form a C=O bond at the radical site, whereas the classical ion does not react.[28]

The protonated heteroatoms of distonic ions can participate in hydrogen bonding. Such hydrogen-bonded complexes can be intermediates in ion dissociation.[29−35] Distonic ions can also form stable complexes, such as $OHC^{\bullet}{=}OH^+\cdot\cdot OH_2$,[36] ${}^{\bullet}CH_2OH_2^+\cdot\cdot OH_2$,[37] ${}^{\bullet}CH_2OH_2^+\cdot\cdot O(H)CH_3$,[38] ${}^{\bullet}CH_2CH_2O(H)H^+\cdot\cdot O(H)CH_2CH_3$,[39] and such complexes can be identified, for example, by ligand exchange reactions.[40]

Although hydrogen-bonded complexes of distonic ions seem to be common, their energetics have not been well characterized experimentally. Some authors compared the energies of these hydrogen bonds to bonds formed by protonated ions and applied proton affinity correlations[41,42] to estimate the bond strength.[36,39,43,44] These estimates assume that a remote radical site affects neither the proton affinity at the heteroatom nor the hydrogen bond formed with a neutral ligand after the site is protonated. The first assumption is consistent with calculations that show that a remote radical site does not affect the proton affinity of a heteroatom.[45] However, in relation to the second assumption; the effects of a remote radical site on hydrogen bonds of distonic ions were not investigated.

Radical ions, including distonic species, of aromatic molecules such as benzene$^{\bullet+}$ and pyridine$^{\bullet+}$ are often incorporated into many biologically important molecules in an aqueous environment where the predominant interactions occur with multiple water molecules.[46,47] These ions can also form hydrogen bonds with solvents in nature, for example, in icy grains doped with polycyclic aromatic hydrocarbons that are subjected to ionizing radiation in interstellar dust grains.[48,49] The stepwise hydration of these ions can provide insight into the basic molecular interactions that determine hydrophobic and hydrophilic hydration in macroscopic systems. In a recent paper, we examined such interactions in the benzene$^{\bullet+}$−water system, where the benzene$^{\bullet+}$ ions interact with water molecules by relatively weak carbon-based $CH^{\delta+}\cdot\cdot O$ hydrogen bonds.[50,51] In comparison, pyridine radical ions can form distonic isomers containing the NH^+ group that can form stronger hydrogen bonds with water molecules.[52] Moreover, the strong $NH^+\cdot\cdot O$ hydrogen bonds of these ions with water molecules can further stabilize the distonic structures.

To better understand the interactions of distonic ions with solvents, the thermochemistry of these interactions need to be characterized. In the present work, we apply equilibrium studies to study the hydration of distonic ions. Namely, we shall look at the stepwise solvation of pyridine$^{\bullet+}$ and 2-fluoropyridine$^{\bullet+}$ (2-F-pyridine$^{\bullet+}$) by several H_2O molecules, and compare the thermochemistry with the solvation of other radical and even-electron ions. This work aims to establish a unified molecular level understanding of the role of hydrogen bonding interactions in determining the structures of the hydrated conventional radical and distonic ions by comparing the hydration energies and structures of benzene and pyridine radical cations. The results of the present work will (1) provide stepwise solvation energies of distonic ions to several water molecules and determine the structures of the hydrated ions; (2) demonstrate that distonic ions can be identified by their hydrogen bond strengths; (3) show that ionic hydrogen bonds at the protonated site are not affected by the presence a radical center at another site; and (4) show

* To whom correspondence should be addressed. selshall@hsc.vcu.edu (S.E.-S.); m.mautner@eco88.com (M.M.-N.)

10.1021/jp067390h CCC: $37.00
Published on Web 01/20/2007

that the distonic isomers are stabilized by solvation more than the conventional isomers.

II. Experimental Section

The experiments were conducted using the Virginia Commonwealth University (VCU) mass-selected ion mobility spectrometer. The details of the instrument can be found in several publications and only a brief description of the experimental procedure is given here.[51,53,54]

The molecular ions (pyridine$^{\bullet+}$ or 2-F-pyridine$^{\bullet+}$) were generated by electron impact (EI) ionization (using 100−120 eV electrons) of the corresponding neutral molecules following the expansion of 100 psig (6.9 bars) of ultra pure helium seeded with a 0.1% of pyridine or 2-F-pyridine vapor through a pulsed nozzle into a vacuum chamber (10^{-7} mbar). To form the protonated or the deutrated species, the pyridine or 2-F-pyridine vapor was coexpanded with methanol or CD_3OD and the mixed neutral clusters were ionized by EI. In all cases, the molecular ions of interest were mass selected in a quadrupole mass filter and injected (in 5 −15 μs pulses) into a drift cell (the inner diameter and length of the total cell are 8.1 and 8.9 cm, respectively) filled with ~0.27 mbar of neat H_2O vapor. Flow controllers (MKS # 1479A) were used to maintain a constant pressure inside the drift cell. The temperature of the drift cell can be controlled to better than ±1 K using six temperature controllers. The injected ions reacted with water and the equilibrium was quickly established. The equilibrium reactants and products drifted through the cell under the effect of weak electric field to the exit plate of the cell. The ions were then analyzed and detected by a second quadrupole mass filter. The arrival time distributions of the ions (ATDs) were collected by monitoring the intensity of each ion as a function of time. The establishment of the equilibrium was verified by two criteria: (1) the ratio of the product to reactants did not change as the reaction time was changed by varying the drift voltage and (2) the reactants and products had equal arrive times indicating equal residence time.

The equilibrium constants K for stepwise clustering reactions (1) were determined from eq 2

$$C_5H_5N^{\bullet+}(H_2O)_{n-1} + H_2O = C_5H_5N^{\bullet+}(H_2O)_n \qquad (1)$$

$$K = \frac{[C_5H_5N^{\bullet+}(H_2O)_n]}{[C_5H_5N^{\bullet+}(H_2O)_{n-1}][H_2O]} = \frac{I_{C_5H_5N^{\bullet+}(H_2O)_n}}{I_{C_5H_5N^{\bullet+}(H_2O)_{n-1}} P_{H_2O}} \qquad (2)$$

The intensities I of the reactants and products were obtained by integrating the ATDs. The equilibrium constant was measured at different temperatures and from the van't Hoff plots the $\Delta H°$ and $\Delta S°$ were obtained from the slope and intercept, respectively (Note units: 1 kcal/mol = 4.184 kJ/mol). The estimated uncertainties based on standard deviations of the slopes and intercepts of the van't Hoff plots, and the reproducibility of cluster data from various sources are $\Delta H°_{n-1,n}$ ± 1.0 kcal mol^{-1} and $\Delta S°_{n-1,n}$ ± 2 cal mol^{-1} K^{-1}.

III. Theoretical Calculations

Ab initio calculations were performed using GAUSSIAN03 package.[55] The structures of all species were fully optimized at the ROHF/6-31+G** level (all electrons are restricted to pairs except one). The binding energies were calculated at the MP2//ROHF/6-31+G** level (single point MP2 calculation at the ROHF/6-31+G** optimized geometry). Binding energies were corrected for basis set superposition error (BSSE) by the counterpoise procedure as implemented in the GAUSSIAN03 package. Unscaled zero-point vibrational energy (ZPVE) was also included as described in the Results Section. All the computed values correspond to 0 K.

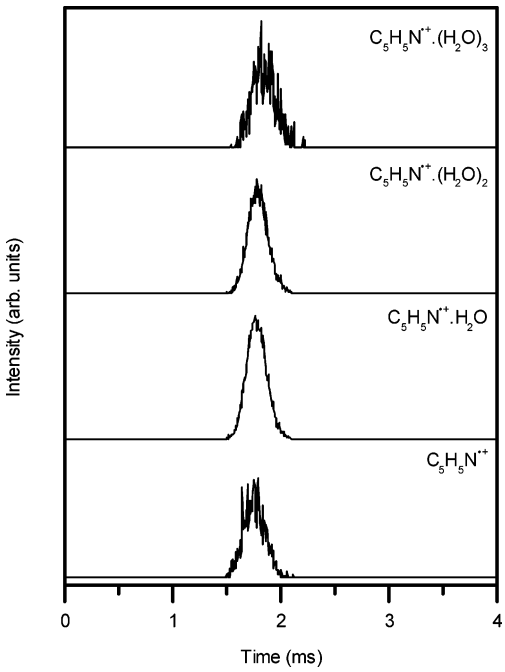

Figure 1. Arrival time distributions of ions formed by the injection of pyridine$^{\bullet+}$ ions (17 eV lab injection energy) into 0.45 mbar H_2O vapor at 304 K.

IV. Results and Discussion

1. Thermochemistry and Structural Implications. For the thermochemical studies, pyridine$^{\bullet+}$ (m/z 79) ions were injected into H_2O or D_2O vapor at 0.27−0.40 mbar in the mobility cell. Through the temperature range of the studies, cluster ions of m/z 79, 97, 115, 133, and 151 (pyridine$^{\bullet+}(H_2O)_n$, n = 0−4) were observed and had equal arrival time distributions as shown in Figure 1, which indicates that they were in equilibrium. Temperature studies of the equilibrium constants yielded the van't Hoff plots shown in Figure 2. The thermochemcial results were independent of the water pressure in this range, and measurements using H_2O or D_2O gave indistinguishable results within experimental accuracy ($\Delta H°_{n-1,n}$ ± 1.0 kcal mol^{-1}, $\Delta S°_{n-1,n}$ ± 2 cal mol^{-1} K^{-1}).

Table 1 shows the thermochemistry of the hydrated clusters of the pyridine$^{\bullet+}$ and 2-F-pyridine$^{\bullet+}$ radical cations, and for comparison also of benzene$^{\bullet+}$ and of the protonated pyridineH^+ ion.

In relation to these data, note that the C−H hydrogens of the conventional $C_5H_5N^{\bullet+}$ (pyridine$^{\bullet+}$) radical cation can only form carbon-based $CH^{\delta+}\cdot\cdot OH_2$ bonds to water, similar to those formed by the $C_6H_6^{\bullet+}$ (benzene$^{\bullet+}$) ion.[50,51] Such hydrogen bonds are typically weak, about 8−12 kcal mol^{-1}.[52,56] In fact, the ab intio calculations below also show that the hydrogen bond strength of the conventional pyridine$^{\bullet+}$ ion to H_2O is 10.2 kcal/mol, similar to the 9.0 kcal/mol bond of benzene$^{\bullet+}(H_2O)$.[50,51] In contrast, the distonic $^{\bullet}C_5H_4NH^+$ structure that is protonated on nitrogen forms a stronger conventional $NH^+\cdot\cdot OH_2$ bond similar to the $C_5H_5NH^+(H_2O)$ complex of protonated pyridine.

These relations can be used to examine the structure of the ion. The results in Table 1 show that the binding enthalpies of pyridine$^{\bullet+}(H_2O)_n$ are equal to those of pyridine$H^+(H_2O)_n$ within the uncertainty of ±1.0 kcal mol^{-1}. In both series, $-\Delta H°_{n-1,n}$

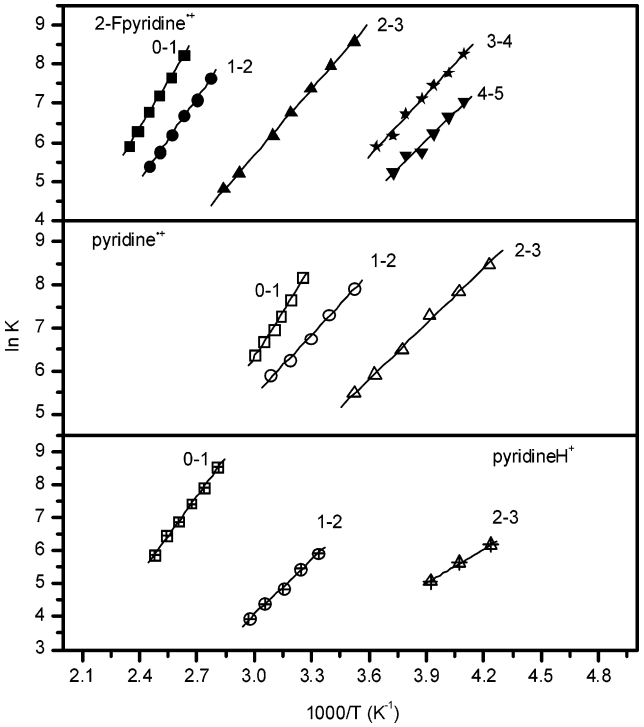

Figure 2. van't Hoff plots for the association equilibria $B(H_2O)_{n-1} + (H_2O) = B(H_2O)_n$ for the ions B = 2-F-pyridine$^{\bullet+}$, pyridine$^{\bullet+}$, and pyridineH^+ as shown.

TABLE 1: Experimental Thermochemistry of the Stepwise Binding Enthalpies $-\Delta H°_{n-1,n}$ and Entropies $-\Delta S°_{n-1,n}$ of H_2O Molecules to Different Ions[a]

	pyridine$^{\bullet+}$		2-F-pyridine$^{\bullet+}$		pyridineH^+		benzene$^{\bullet+}$[b]	
n	$-\Delta H°$	$-\Delta S°$	$-\Delta H°$	$-\Delta S°$	$-\Delta H°$	$-\Delta S°$	$-\Delta H°$	$-\Delta S°$
1	15.2	33.1	16.0	25.7	15.6 (15.0[c],16.1[d])	27.0 (25.5[c], 27.0[d])	9.0	19.5
2	9.9	19.0	13.6	22.4	11.5 (9.6[c])	26.0 (19.6[c])	8.0	18.9
3	8.8	20.2	11.3	22.3	6.9 (8.3[c])	17.1 (19.6[c])	8.0	
4	7.1	15.3	10.4	25.5			10.3	22.4
5			9.7	25.4			8.6	18.1
6			8.9[e]				7.8	15.1

[a] Units: $\Delta H°$ (kcal/mol), $\Delta S°$ (cal/mol K). Estimated uncertainties based on standard deviations of the slopes and intercepts of van't Hoff plots, and reproducibility of cluster data from various sources: $\Delta H°_{n-1,n} \pm 1.0$ kcal mol^{-1}, $\Delta S°_{n-1,n} \pm 2$ cal mol^{-1}K^{-1}. [b] References 50, 51. [c] Reference 63. [d] Reference 64. [e] From measured $\Delta G°$ assuming $\Delta S° = -25.0$ cal mol^{-1} K^{-1}.

decrease similarly with increasing n and approach and somewhat undershoot the limiting macroscopic value of 10.5 kcal mol^{-1} of condensation energy of water. This follows the usual trend in systems with conventional ionic hydrogen bonds.[52,56] The clusters of 2-F-pyridine$^{\bullet+}$ also show similar binding energy for the first H_2O molecule and decreasing bonding energy with n, except for somewhat stronger bonds to further water molecules, possible by direct interactions with the fluorine atom.

In contrast, Table 1 shows that the binding energy of the first H_2O molecule is smaller in benzene$^{\bullet+}(H_2O)_n$[51,52] and $\Delta H°_{n-1,n}$ changes little with increasing n, in a manner characteristic to other $CH^{\delta+}\cdot\cdot(OH_2)_n$ systems such as $(CH_3)_4N^+(H_2O)_n$.[57] The cluster distributions in benzene$^{\bullet+}(H_2O)_n$ were also unusual and different from that in pyridine$^{\bullet+}(H_2O)_n$, showing two groups, $n = 0-2$ and $n = 3-8$, with a minimum at $C_6H_6{}^{\bullet+}(H_2O)_3$ due to the deprotonation to form $(H_2O)_nH^+$ clusters.[50,51]

The pyridine$^{\bullet+}(H_2O)_n$ clusters and the 2-F-pyridine$^{\bullet+}(H_2O)_n$ clusters therefore show binding energies and cluster distributions

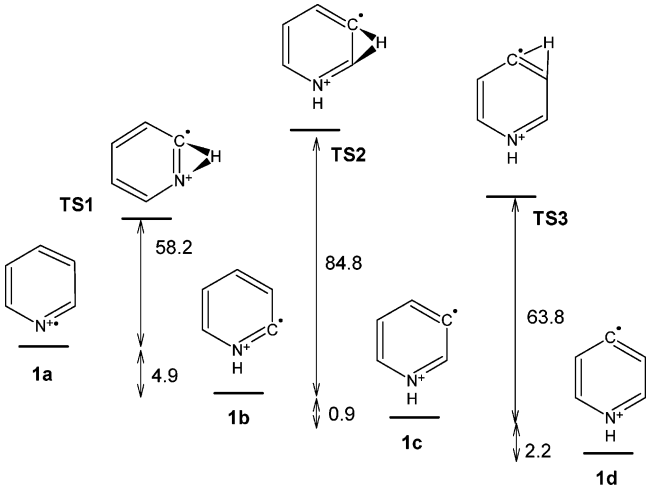

Figure 3. Potential energy diagram for conventional pyridine$^{\bullet+}$, distonic isomers, and the transition states for the hydrogen shift. Energies are kcal/mol at MP2//ROHF-6-31+G** level (corrected for ZPE).

similar to pyridine$H^+(H_2O)_n$ where water is bonded by an $NH^+\cdot\cdot\cdot OH_2$ bond. This indicates that pyridine$^{\bullet+}$ and 2-F-pyridine$^{\bullet+}$ contain protonated nitrogen corresponding to the distonic $^{\bullet}C_5H_4$-NH^+ and $^{\bullet}C_5H_3FNH^+$ structures. The results are not compatible with the classical $C_5H_5N^{\bullet+}$ and $C_5H_4FN^{\bullet+}$ structures that would form weaker benzene$^{\bullet+}$ like $CH\cdots OH_2$ bonds.

As a result of the stronger $NH^+\cdots OH_2$ vs $CH^{\delta+}\cdots OH_2$ bonds the thermochemistry of the conventional → distonic ion rearrangement becomes more favorable by solvation. Using the benzene$^{\bullet+}(H_2O)_n$ clusters as models for the conventional ion, the data in Table 1 shows that the difference between the total solvation energies (sum of the stepwise energies shown in Table 1) of the pyridine$^{\bullet+}(H_2O)_n$ and the benzene$^{\bullet+}(H_2O)_n$ ions is 6.2, 8.1, and 8.9 kcal mol^{-1} for $n = 1-3$, respectively. Using the theoretical difference between the energies of the unsolvated ions (shown in Figure 3), the distonic ion (1d) is then more stable by 8.0, 14.2, 16.1, and 16.9 kcal mol^{-1} than the classical ion (1a) when they are unsolvated or solvated by one, two, or three H_2O molecules, respectively.

As to the formation of the distonic ions, electron impact ionization of pyridine generates the conventional ion.[28] These ions could rearrange to the distonic structures upon energetic collisions when injected into the drift cell. Figure 3 shows barriers to H shift up to 84.8 kcal/mol (3.7 eV) and previous calculations showed barriers of 60−70 kcal/mol for H shifts among the isomers.[8] These barriers could be overcome by the 17 eV (392 kcal/mol) injection energy (the background pressure in this region is 10^{-5} mbar). However, the isomers react differently in 5 eV collisions with H_2O and other molecules, apparently retaining their distinct structures.[28]

A more likely mechanism for forming the distonic ion is by proton transfer catalysis assisted by neutral ligand molecules.[58] This can occur in ionized pyridine clusters in which we generate the ions, or in interactions in the reaction cell. In this mechanism, proton transfer to a ligand can lower the barrier to interconversion between isomers. For example, this mechanism was observed in $HCN^{\bullet+}/HNC^{\bullet+}$ catalyzed by CO,[59] in HCO^+/HOC^+ catalyzed by Ar and N_2;[60] and in the conventional/distonic pair $CH_3OH^{\bullet+}/^{\bullet}CH_2OH_2^+$ catalyzed by H_2O.[61] Also, hydrogen bonding to a ligand can decrease the barrier to rearrangement.[39]

In our case conventional $C_5H_5N^{\bullet+}$ ions may transfer a proton to H_2O in the excited $[C_5H_5N^{\bullet+}(H_2O)_n]^*$ clustering reaction intermediates, forming $[^{\bullet}C_5H_4N\cdot\cdot H^+(H_2O)_n]^*$ which yield the

TABLE 2: Stepwise Binding Energies of H_2O Molecules to Ions at MP2//ROHF/6-31+G Corrected for ZPE and BSSE[a]**

	pyridine$^{\bullet+}$				2-F-pyridine$^{\bullet+}$		pyridineH$^+$	2-F-pyridineH$^+$
		$^{\bullet}C_5H_4NH^+$ (distonic)[b]						
n	$C_5H_5N^{\bullet+}$ (conventional)	1b	1c	1d	$C_5H_4FN^{\bullet+}$ (conventional)	$^{\bullet}C_5H_3FNH^+$ (distonic)	$C_5H_5NH^+$	$C_5H_4FNH^+$
1	−10.2	−15.4	−15.0	−15.4	−10.0	−15.9	−14.5	−15.5
				(−15.2)		*(−16.0)*	*(−15.6)*	
2		−10.3		−10.2			−9.9	−10.3
				(−9.9)			*(−11.5)*	
3				−8.7				
				(−8.8)				

[a] Experimental values in italics. Units are kcal mol^{-1}. [b] The numbering refers to the position of the radical relative to the nitrogen atom, see Figure 6.

$^{\bullet}C_5H_4NH^+(H_2O)_n$ distonic clusters. In the analogous benzene$^{\bullet+}$-$(H_2O)_n$ clusters ($n = 1-4$) we calculated barriers of 43, 33, 28, and 26 kcal/mol for the intracluster proton transfer from carbon to water,[51] a reaction that is similar to the first intracluster proton transfer in the pyridine$^{\bullet+}$/water clusters. These barriers are significantly smaller than the calculated 60−80 kcal/mol barriers for C to N shift in unsolvated pyridine$^{\bullet+}$ ion. This mechanism can therefore reduce the barrier for the conventional → distonic rearrangement.

We also note that in our experiments we ionize pyridine clusters formed in supersonic jet expansion, and similar conventional → distonic rearrangement may be catalyzed by neutral pyridine molecules in the clusters already when the ions are formed by electron impact.

In summary, solvation can facilitate the conversion from the conventional to the distonic ion kinetically by decreasing barriers to rearrangement, and thermochemically by making the overall process more exothermic.

2. Theoretical Results. 2a. Energies of the Unsolvated Ions, and Proton Affinities. The energies of the species calculated are shown in Table 2 and the structures are shown in Figures 4−6. Three distonic isomers (**1b**, **1c**, **and 1d**) were considered for the pyridine radical cation as shown in Figure 3. The energies calculated at MP2//ROHF/6-31+G** (corrected for ZPE) indicated that the distonic isomer **1d** is more stable than isomers **1b** and **1c** by 3.1 and 2.2 kcal/mol, respectively. This is consistent with previous studies which showed that isomer **1d** is more stable than **1b** and **1c** distonic isomers by 3 and 2 kcal/mol, respectively, at the B3LYP/6-31G** (corrected for ZPE) level.[8] In addition, the distonic isomer **1d** is calculated to be more stable than the conventional pyridine radical cation by 8.0 kcal/mol at MP2//ROHF/6-31+G** (corrected for ZPE). Our calculations at MP2//ROHF/6-31+G** level (corrected for ZPE) suggests energy barriers of 58.2 (**1a**−**1b**), 84.8 (**1b**−**1c**), and 63.8 (**1c**−**1d**) kcal/mol as indicated in Figure 3 for the consecutive shifts of H atoms that convert the isomers. These barriers can be easily accessed in the electron impact ion source that uses 70−100 eV (1614−2306 kcal/mol) electrons.

We also calculated the proton affinities of some of the species in these systems. The proton affinity (PA) was calculated from the energy change of the following reaction: $XH^+ \rightarrow X + H^+$ where the energy of the proton is taken as zero. The energies of X and XH^+ species were taken from the MP2//ROHF/6-31+G** calculations (0 K) corrected for the ZPVE. The calculated PAs of pyridine and 2-F-pyridine are 220 and 208 kcal/mol, respectively, which are slightly lower than the tabulated experimental values of 222 and 211 kcal/mol (with an uncertainty of ±1.5 kcal/mol in the tabulated values).[62] We also calculated a PA of 208 kcal/mol for the conventional pyridine$^{\bullet+}$ ion (i.e., deprotonation energy of $C_5H_4N^{\bullet+}$ on the para-C carbon) and 216 kcal/mol for the distonic pyridine$^{\bullet+}$ ion (i.e., deprotonation energy of $^{\bullet}C_5H_4NH^+$ on N). For 2-F-pyridine, we calculated similarly PA of 198 kcal/mol for the conventional and 205 kcal/mol for the distonic ion.

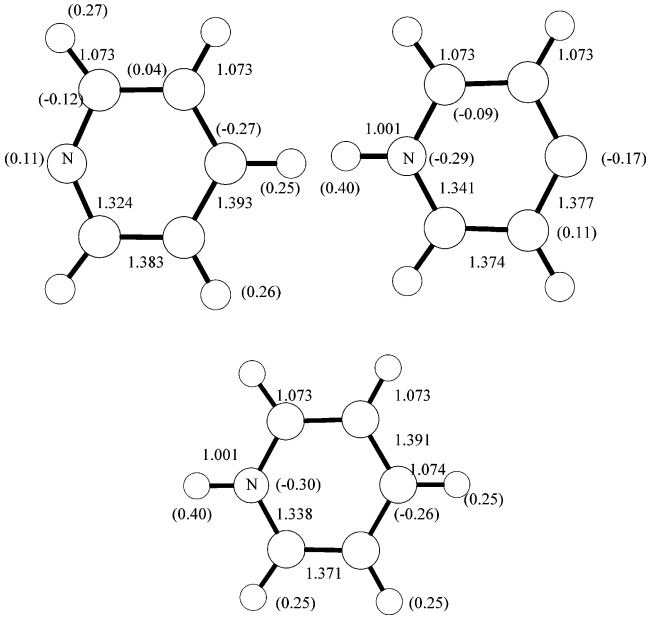

Figure 4. Optimized structures of the conventional (upper left) and distonic (upper right) isomers of pyridine$^{\bullet+}$ and of pyridineH$^+$ (bottom), calculated at the ROHF/6-31+G** level. Distances are in Angstrom (1 Angstrom = 0.1 nm) and atomic charges are in parentheses. Note the similarities between the atomic charges and bond distance about the NH^+ centers in the protonated and distonic ions.

The calculated deprotonation energy of 208 kcal/mol of the classical pyridine$^{\bullet+}$ ion on C, when adding the 2−3 kcal/mol underestimate of PA in these calculations, is in excellent agreement with the experiment-based deprotonation energy of 211 kcal/mol of benzene$^{\bullet+}$ on C. This shows that the C−H bonds on benzene$^{\bullet+}$ and pyridine$^{\bullet+}$ are similar, in support of the arguments below.

2b. Energies of the Solvated Ions. Figure 5 shows the clusters of the protonated pyridineH$^+$ ion and of the distonic ion with 1 and 2 H_2O molecules. The calculated $CH^{\delta+}\cdot\cdot OH_2$ binding energy for the conventional pyridine ion to one water molecule is 10.2 kcal/mol (Table 2), which does not agree with the experimental measured value of 15.6 kcal/mol (Table 1), while the calculated $NH^+\cdot\cdot OH_2$ binding energy of the distonic pyridine ion to one water molecule is 15.4 kcal/mol, in excellent agreement with the experimental measured value of 15.6 kcal/

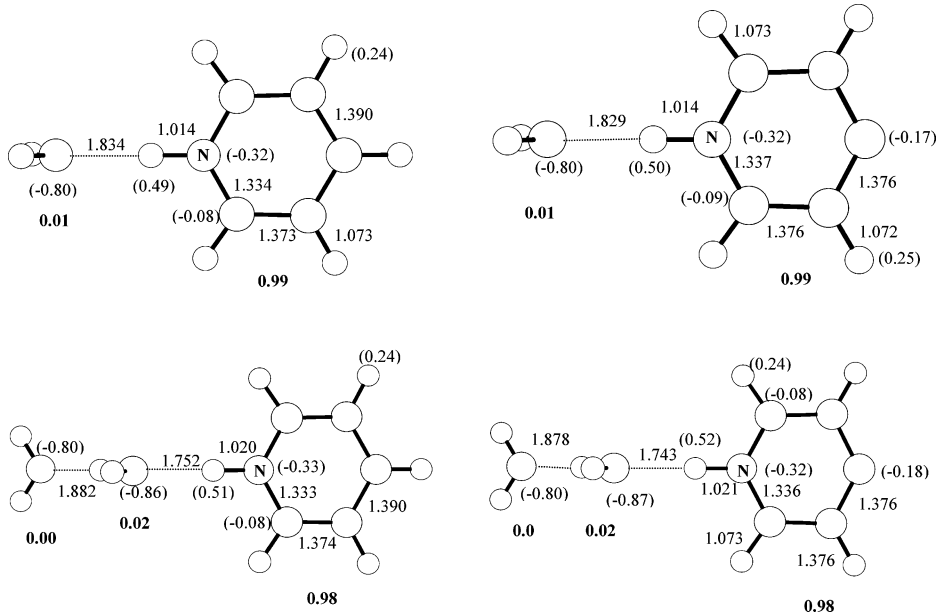

Figure 5. Optimized structures of $C_5H_5NH^+(H_2O)_{1,2}$ (left) and $C_5H_4NH^{\bullet+}(H_2O)_{1,2}$ (right) at ROHF/6-31+G** level. Distances are in Angstrom, molecular charges are in Bold, and atomic charges are in parenthesis. Note the similarities between the bond lengths and atomic and group charges of the bonds and ligands in the respective clusters of the protonated and distonic ions.

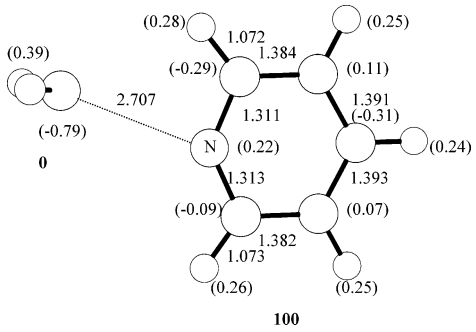

Figure 6. Optimized structures of $C_5H_5N^{\bullet+}H_2O$ (hydrated conventional pyridine$^{\bullet+}$ isomer) ion at ROHF/6-31+G** level. Distances are in Angstrom, molecular group charges are in Bold, and atomic charges are in parenthesis.

mol. This is also close to the bonding energy of one H_2O molecule to the protonated pyridineH^+ ion.

The binding energies for the addition of one water molecule to the three distonic isomers (**1b**, **1c**, **and 1d**) are effectively equal as shown in Table 2, and because the unhydrated isomers themselves are also close in energy, a mixture of the hydrated isomers may also exist in the experiment. Because both the unhydrated and singly hydrated isomer **1d** is slightly more stable than the other two, all the subsequent calculations on the distonic ion were done assuming isomer **1d**.

As noted above, the difference in stabilization energy between the distonic pyridine cation (**1d**) and the conventional ion (**1a**) increases upon association with one water molecule because of the stronger bonding of the water molecule to the distonic ion. Using the calculated energies in Table 2, the stabilization increases from 8.0 to 13.2 kcal/mol, close to the experiment-based 14.2 kcal/mol in the preceding section.

Figure 5 also shows the cluster of the distonic ion with two H_2O molecules. The water molecules are bonded to N−H hydrogen atoms and they have similar but somewhat higher energies. The formation of isomers with similar energies is common in hydrogen-bonded clusters and the observed populations may include equilibrium mixtures of isomers. Again, an excellent agreement is obtained for the addition of the second water molecule to the distonic pyridine (10.2 kcal/mol) with that measured experimentally as 9.9 kcal/mol (Table 1). These binding energies also agree with the calculated and experimental values for the corresponding protonated pyridine ion (Tables 1 and 2).

2c. Structures and Charge Distributions. Figure 4 shows the ab initio structures and charge distributions of the conventional and distonic pyridine$^{\bullet+}$ radical ion and of the protonated (pyridineH^+) ion. Of interest with respect to clusters is comparing the hydrogen-bonding N−H^+ centers in the distonic pyridine, $^{\bullet}C_5H_4N-H^+$, and protonated pyridine, $C_5H_5N-H^+$, ions. Figure 4 shows that the geometries around the N−H^+ group, the lengths of this bond and the neighboring C−N, and C−H bonds are virtually identical. The charges on the proton and nitrogen of the distonic ion are also identical to those in the protonated ion. This is important because these charges affect the hydrogen bonds, and their similarity accounts for the similar hydrogen bond strengths of the two ions to water. In contrast, the charges on the C−H hydrogens of the conventional ion are significantly smaller at 0.25−0.27 unit charge, which accounts for the smaller binding energies to an H_2O molecule.

Figure 5 shows that the similarity of the distonic and protonated pyridine$^{\bullet+}$ ions also applies in their complexes with one and two H_2O molecules. Here again the bond lengths and charges about the hydrogen bonds are similar in the complexes of these ions. On the other hand, the structure of the conventional $C_5H_5N^{\bullet+}$ bound to one water molecule shown in Figure 6 is different. In the most stable adduct the H_2O molecule is bonded by a long noncovalent bond (2.707 Å) to the positively charged nitrogen. Another isomer with a $C-H^{\delta+}\cdot\cdot OH_2$ bond and an isomer with a bifurcated bond to two CH hydrogens, similar to a structure we found in $C_6H_6^{\bullet+}(OH_2)$,[50,51] are also close in energy.

For all the ions, Figures 5 and 6 show that solvation by one or two H_2O molecules moves little of the ionic charge. In the conventional distonic and protonated ions, 98% - 100% of the charge remains on the pyridine ions.

2d. Calculations for 2-F-pyridine. For 2-F-pyridine$^{\bullet+}$, the conventional ion (Figure 7, isomer 2a) and four distonic isomers

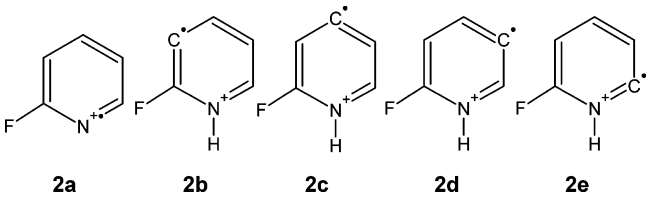

Figure 7. Isomers of the conventional (a) and distonic (b−e) isomers of the 2-F-pyridine$^{\bullet+}$ ion.

were considered (Figure 7, isomers 2b−e) were considered. Similar to the pyridine distonic ion, isomer **2c** was found to be more stable than isomers **2b**, **2d**, and **2e** by 4.3, 2.3, and 3.4 kcal/mol, respectively. The distonic ion isomer **2c**, as in pyridine, is more stable than the corresponding conventional ion **2a** by 6.5 kcal/mol. The difference increases to 13.6 kcal/mol upon clustering with one water molecule because of the stronger bonding of the distonic ion to water.

The geometrical parameters around the N−H site in both the distonic ion **2c** and that in protonated 2-F-pyridineH$^+$ are also identical. This applies also in the similarity of the structures of $^{\bullet}C_5H_3FNH^+(H_2O)$ (distonic) and $C_5H_4FNH^{\bullet+}(H_2O)$ (protonated) in Figure 8. The calculated binding energies are also similar, 15.9 kcal/mol for $^{\bullet}C_5H_3FNH^+(H_2O)$ (distonic) and 15.5 kcal/mol for $C_5H_4FNH^+(H_2O)$ which are different from the 11.3 kcal/mol binding energy in the corresponding $C_5H_4FN^{\bullet+}(H_2O)$ conventional ion. This again supports, as in the case of pyridine, the conclusion that the experimentally measured binding energy corresponds to the distonic rather than the conventional ion.

Figure 8 shows that the F atom has significant negative charge in the conventional, and even more in the distonic ion. The figure also shows that the first H_2O molecule does not interact significantly with this charge, and therefore the F substitution does not affect significantly the calculated binding energy of H_2O to distonic 2-F-pyridine$^{\bullet+}$ compared with distonic pyridine$^{\bullet+}$ as well as with pyridineH$^+$ and 2-F-pyridineH$^+$ ions. However, the further H_2O molecules can form N−H$^+$··OH$_2$·· O(H)H··F− cyclic structures by hydrogen bonding to fluorine, which may account for the increased binding energies in the 2-F-pyridine$^{\bullet+}(H_2O)_n$ vs pyridine$^{\bullet+}(H_2O)_n$ and pyridineH$^+$-$(H_2O)_n$ ($n = 2-4$) clusters (Table 1).

3. Further Reactions with Water Vapor: Hydrogen Transfer, H/D Exchange, and Proton Abstraction. The ions and clusters in this study may react with water vapor in several ways: hydrogen extraction, deprotonation in clusters, and full deprotonation. The reactivities allow further probes of classical vs distonic structure.

3a. Hydrogen Transfer from Water. The identity of the pyridine$^{\bullet+}$ ion can be tested by reaction with water vapor. This

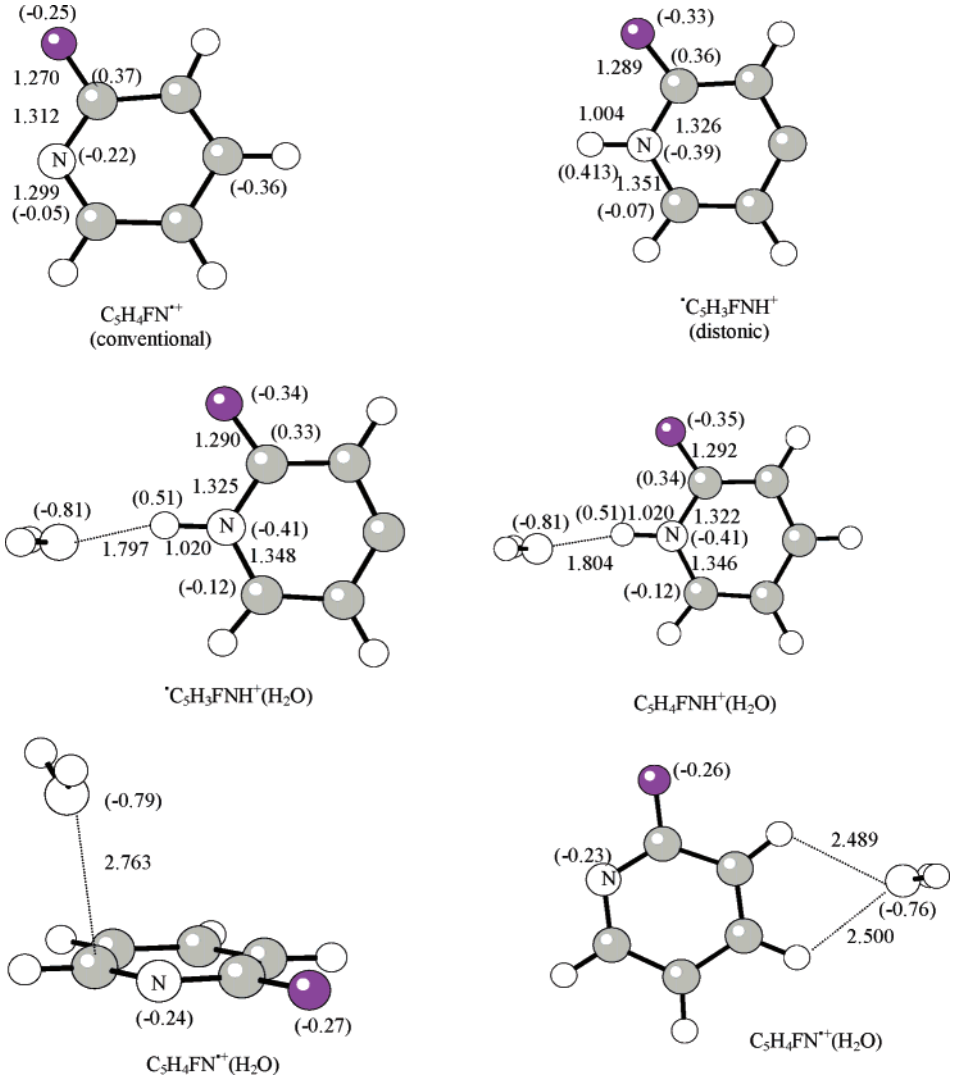

Figure 8. Optimized structures of $C_5H_4FN^{\bullet+}$ (2-F-pyridine$^{\bullet+}$) (conventional and distonic), and the adducts of the ions with one H_2O molecule: distonic radical ion (middle left), protonated ion (middle right), and two isomers of the conventional radical ion (bottom) at the ROHF/6-31+G** level.

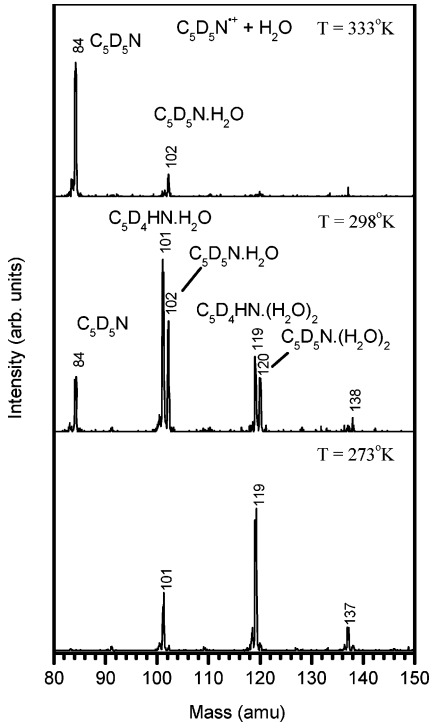

Figure 9. Mass spectra of pyridine-$D_5^{\bullet+}$ (*m*/*z* 84) injected into H_2O vapor. P(H_2O) = 0.34 mbar (298°K), injection energy = 17 eV (lab frame). (Top) Note the absence of $C_5H_5NH^+$ ions, indicating that the ion does not extract H atoms from H_2O, and the absence of H/D exchange product at *m*/*z* 101 at 333 K. Center and bottom panels: Note the presence of both nonexchanged and exchanged ions at *m*/*z* 101, 102; 119, 120, at 298 K, indicating some intra-cluster proton transfer and consequent slow H/D exchange with water vapor at 298 K, and faster H/D exchange at 273 K leaving only exchanged ions. Also note the absence of $(H_2O)_nH^+$ ions indicating that the ions are not deprotonated by water vapor to form protonated water clusters.

test relies on the energy difference between the classical and distonic isomers. Using the theoretical results and tabulated ion energetics,[62] we can calculate that reaction 3 of the conventional ion would be exothermic by 2 kcal/mol. This is within the uncertainty of the thermochemical data, but if indeed exothermic, such reactions are usually fast and would go to completion in about 10^{-7} s under our conditions, much faster than our millisecond observation times. To test the reactivity, we injected pyridine-$D_5^{\bullet+}$ ions (*m*/*z* 84) into H_2O vapor in the ion mobility cell.

$$C_5D_5N^{\bullet+} + H_2O \rightarrow C_5D_5NH^+ + OH^{\bullet} \qquad (3)$$

Figure 9, top panel, shows that the unsolvated ions (*m*/*z* 84) did not abstract H atoms from H_2O as the product $C_5D_5NH^+$ ions (*m*/*z* 85) are not observed. The results are consistent with the distonic structure that is expected not to be reactive.

3b. Intra-Cluster Proton Transfer and H/D Exchange. If the proton is transferred from the core ion to water molecules in a hydrated cluster, the resulting $(H_2O)_nH^+$ moiety with a labile proton can exchange hydrogen with D_2O vapor. Figures 9−11 show tests of H/D exchange for hydrated clusters of several ions, using various isotopic labeling. For the distonic pyridine$^{\bullet+}$-D_5 ion, reaction 4 describes the H/D exchange reaction.

$$C_5D_4ND^+(H_2O)_n + H_2O \rightarrow {}^{\bullet}C_5D_4N[(H_2O)_nD^+] + H_2O \rightarrow C_5D_4N[(H_2O)_nH^+] + HDO \qquad (4)$$

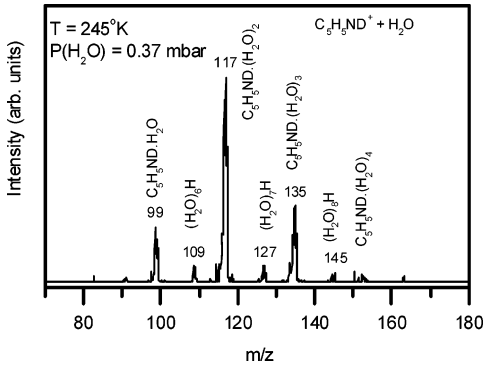

Figure 10. Injection of protonated pyridine (here, the deuterium labeled $C_5H_5ND^+$ ion), into H_2O vapor to test H/D exchange and deprotonation of the ions. (Injection energies of 17 eV lab). Only $C_5H_5ND^+(H_2O)_n$ clusters produced but not exchanged $C_5H_5NH^+(H_2O)_n$ clusters. The minor water clusters observed are possibly from high-energy injection processes. The results show that pyridineH^+ does not undergo intracluster proton transfer to water or overall deprotonation by water.

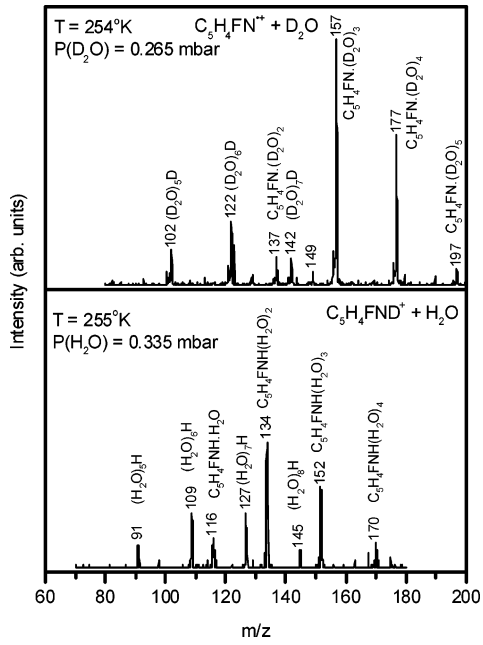

Figure 11. Injection of 2-F-pyridine$^{\bullet+}$ into D_2O vapor (top) and of 2-F-pyridineD^+ into H_2O vapor (bottom panel) at injection energies of 17−20 eV (lab). (Top) 2-F-pyridine$^{\bullet+}$ $(D_2O)_n$ ions do not undergo H/D exchange to form ${}^{\bullet+}C_5H_3ND^+(D_2O)_n$ ions, indicating no intracluster proton transfer. However, the water clusters $(D_2O)_nD^+$ indicate overall deprotonation by water. (Bottom) Injection of protonated (D labeled) 2-$FC_5H_4ND^+$ into H_2O vapor produces the exchanged 2-$FC_5H_4NH^+$-$(H_2O)_n$ clusters indicating D/H exchange and intracluster proton transfer, and the $(H_2O)_nH^+$ clusters indicating overall deprotonation.

The D/H exchange would convert the *m*/*z* 84, 102, 120, and 138 ions (n = 0−3) to *m*/*z* 83, 101, 119, and 137 ions, respectively. However, Figure 9, top panel, shows that no exchange occurs at 333 K where only the unsolvated and singly hydrated ions are present, indicating that in these ions the deuteron remains bonded to pyridine.

However, intra-cluster proton transfer to water becomes more favorable in larger clusters, where producing a strong hydrogen-bond network in $(H_2O)_nH^+$ can drive proton transfer to water. Correspondingly, Figure 9, middle and bottom panels, show that as the population of the *n* = 3 cluster (*m*/*z* 138) grows with decreasing temperature, the D/H exchanged ions appear, and at lower temperatures only the exchanged clusters are observed.

These observations in pyridine$^{\bullet+}(H_2O)_n$ may be compared with benzene$^{\bullet+}(H_2O)_n$ that we studied recently,[50,51] and with the protonated pyridine$H^+(H_2O)_n$ clusters that we studied here (Figure 10). None of these ions undergo H/D exchange reactions with water vapor under any conditions, indicating the absence of intra-cluster proton transfer. In benzene$^{\bullet+}(H_2O)_n$ this may be attributed to a barrier to dissociating a C−H bond,[50,51] and in pyridine$H^+(H_2O)_n$ to the high deprotonation energy of 222 kcal/mol at the nitrogen center. In comparison, the calculated deprotonation energy of NH^+ of the distonic pyridine$^{\bullet+}$ ion is somewhat lower, 216 kcal/mol, which allows the intra-cluster proton transfer and consequent H/D exchange, as observed.

3c. Overall Deprotonation. Finally, water vapor can fully deprotonate ions to form $(H_2O)_nH^+$ clusters. We found that benzene$^{\bullet+}$ and 2-F-pyridineH^+ both can be deprotonated, consistent with the relatively low proton affinity of 212 kcal/mol of $C_6H_5^\bullet$ and 2-F-pyridine. In comparison, pyridine has a higher proton affinity of 222 kcal/mol and it is not deprotonated by water vapor.

Here again we can compare pyridine$^{\bullet+}$ with either benzene$^{\bullet+}$ or pyridineH^+. The deprotonation energy of the conventional ion at a C−H bond is calculated as 208 kcal/mol, comparable to C−H deprotonation of benzene$^{\bullet+}$ at 211 kcal/mol. The deprotonation energy of the N−H bond of the distonic ion is calculated as 216 kcal/mol, closer to pyridineH^+. Experimentally, the pyridine$^{\bullet+}$ ion was not deprotonated, consistent with the higher deprotonation energy of the distonic ion, and further supporting the distonic structure.

3d. Observations on 2-F-pyridine. The experimental binding energy of 2-F-pyridine$^{\bullet+}$ to H_2O is 16 kcal/mol, similar to the ab intio calculated binding energy of 15.5 kcal/mol of the protonated 2-F-pyridineH^+ to H_2O. This indicates that 2-F-pyridine$^{\bullet+}$ also has an N-protonated distonic structure that can form an $N-H^+\cdot\cdot OH_2$ bond. For the addition of further H_2O molecules, Table 1 shows stronger bonding energies to 2-F-pyridine$^{\bullet+}$ than to the other core ions. For example, the total binding energy of 2-F-pyridine$^{\bullet+}$ to 3 H_2O molecules is 40.9 kcal/mol, compared with 34 kcal/mol for both pyridineH^+ and pyridine$^{\bullet+}$. Also, we could observe clusters with up to 6 H_2O molecules with 2-F-pyridine$^{\bullet+}$ but only up to 4 H_2O molecules with the other ions. This suggests that the F atom in the ortho position may interact with the water molecules.

With respect to the intracluster proton transfer and H/D exchange, and overall deprotonation, 2-F-pyridine$^{\bullet+}$ also shows somewhat anomalous behavior, when compared with the protonated 2-F-pyridineH^+ counterpart. The ab initio calculated N−H deprotonation energy of the distonic 2-F-pyridine$^{\bullet+}$ ion is 205 kcal/mol, similar to the 208 kcal/mol calculated for 2-F-pyridineH^+. However, 2-F-pyridine$^{\bullet+}$ does not show either intra-cluster proton transfer or overall deprotonation (Figure 11, top panel) while 2-F-pyridineH^+ undergoes both processes (Figure 11, bottom panel). The anomalously strong binding of water in the larger hydrated clusters 2-F-pyridine$^{\bullet+}(H_2O)_n$ may prevent these processes.

Conclusions

We measured the thermochemistry of stepwise hydration of the pyridine$^{\bullet+}$ radical. Comparisons with the benzene$^{\bullet+}$ and with pyridineH^+ ions suggest that pyridine$^{\bullet+}$ has a distonic structure protonated on nitrogen that can form an $NH^+\cdots OH_2$ bond. This agrees with ab initio calculations that show the distonic ion to be the lowest energy isomer. The stability of the distonic vs conventional ion can be enhanced further by the stronger solvation of the distonic isomer.

The similar hydrogen bond energies of pyridine$^{\bullet+}$ and pyridineH^+ to H_2O show that a radical site away from the hydrogen-bonding center has little effect on the hydrogen bond. This verifies that proton affinity correlations established by even-electron protonated ions can estimate hydrogen bond strengths also of distonic ions.[36,39,43,44]

The distonic structure of the pyridine$^{\bullet+}$ ion observed here is consistent with reactivity with respect to intra-cluster deprotonation and overall deprotonation. Comparing the reactions of benzene$^{\bullet+}$, pyridine$^{\bullet+}$, pyridineH^+, 2-F pyridine$^{\bullet+}$, and 2-F-pyridineH^+ with water vapor, we note that the deprotonation energies of the reactive sites differ only by about 10 kcal/mol, yet the reactivities are different. Intra-cluster proton transfer and overall deprotonation therefore seem to be strongly sensitive to the deprotonation energies of the core ions, and to energy barriers and structural effects.

Similar to pyridine$^{\bullet+}$, the heteroatoms are protonated in the distonic, but not in the conventional, ions of other nitrogen and oxygen heterocyclics, of tertiary amines, and of aldehydes, ketones, and ethers. These distonic ions should also form strong ionic hydrogen bonds. These strong hydrogen bonds can affect their chemistry and can be used, as in the present case, to identify the distonic structures.

Acknowledgment. This work was funded by the National Science Foundation (CHE-0414613) and NASA (NNG04GH45G) Grants.

References and Notes

(1) Audier, H. E.; Milliet, A.; Leblanc, D.; Morton, T. H. *J. Am. Chem. Soc.* **1992**, *114*, 2020.
(2) Bouchoux, G.; Coret, N.; Milliet, J.; Remmp, M.; Terlouw, J. K. *Int. J. Mass Spectrom.* **1998**, *180*, 7.
(3) Kimikinen, L. K. M.; Stirk, K. G.; Kentämaa, H. I. *J. Am. Chem. Soc.* **1992**, *114*, 2027.
(4) Kentämaa, H. I. *Org. Mass Spectrom.* **1994**, *29*, 1.
(5) Smith, R. L.; Franklin, R. L.; Stirk, K. M.; Kentämaa, H. I. *J. Am. Chem. Soc.* **1993**, *115*, 10348.
(6) Gronert, S. *Chem. Rev.* **2001**, *101*, 329.
(7) Lavorato, D.; Terlouw, J. K.; Dargel, T. K.; Koch, W.; McGibbon, G. A.; Schwarz, H. *J. Am. Chem. Soc.* **1996**, *118*, 11898.
(8) Lavorato, D. J.; Terlouw, J. K.; McGibbon, G. A.; Dargel, T. K.; Koch, W.; Schwarz, H. *Int. J. Mass Spectrom.* **1998**, *179*−180, 7.
(9) Gerbaux, P.; Barbieux-Flammang, M.; Terlouw, J. K.; Flammang, R. *Int. J. Mass Spectrom.* **2001**, *206*, 91.
(10) Gerbaux, P.; Van Haverbeke, Y.; Flammang, R. *J. Mass Spectrom.* **1997**, *32*, 1170.
(11) Gerbaux, P.; Barbieux-Flammang, M.; Haverbeke, Y. V.; Flammang, R. *Rapid Commun. Mass Spectrom.* **1999**, *13*, 1707.
(12) Yu, S. J.; Holliman, C.; Rempel, D. L.; Gross, M. L. *J. Am. Chem. Soc.* **1993**, *115*, 9676.
(13) Holmes, J. L.; Lossing, F. P.; Terlouw, J. K.; Burgers, P. C. *J. Am. Chem. Soc.* **1982**, *104*, 2931.
(14) Dargel, T. K.; Koch, W.; Lavorato, D. J.; McGibbon, G. A.; Terlouw, J. K.; Schwarz, H. *Int. J. Mass Spectrom.* **1999**, *185/186/187*, 925.
(15) Schalley, C. A.; Hornung, G.; Schroder, D.; Schwarz, H. *Int. J. Mass Spectrom. Ion Processes* **1998**, *172*, 181.
(16) Stirk, K. M.; Kiminkinen, L. K. M.; Kentämaa, H. I. *Chem. Rev.* **1992**, *92*, 1649.
(17) Stirk, K. G.; Kentämaa, H. I. *J. Am. Chem. Soc.* **1991**, *113*, 5880.
(18) Stirk, K. M.; Orlwski, J. C.; Leeck, D. T.; Kentämaa, H. I. *J. Am. Chem. Soc.* **1992**, *114*, 2027.
(19) Kimikinen, L. K. M.; Stirk, K. G.; Kentämaa, H. I. *J. Am. Chem. Soc.* **1992**, *114*, 8604.
(20) Beasley, B. J.; Smith, R. L.; Kentämaa, H. I. *J. Mass Spectrom.* **1995**, *30*, 384.
(21) Nelson, E. D.; Li, R. M.; Kentämaa, H. I. *Int. J. Mass Spectrom.* **1999**, *187*, 91.
(22) Nelson, E. D.; Thoen, K. K.; Kentämaa, H. I. *J. Am. Chem. Soc.* **1998**, *120*, 3792.
(23) Heldbrink, J. L.; Thoen, K. K.; Kentämaa, H. I. *J. Org. Chem.* **2000**, *65*, 645.

(24) Tichy, S. E.; Hill, B. T.; Campbell, J. L.; Kentämaa, H. I. *J. Am. Chem. Soc.* **2001**, *123*, 7923.
(25) Karapanayiotis, T.; Dimopoulos-Italiano, G.; Bowen, R. D.; Terlouw, J. K. *Int. J. Mass Spectrom.* **2004**, *236*, 1.
(26) Wantier, P.; Bury, M.; De Meyer, C.; Finet, D.; Van Haverbeke, Y. *European J. Mass Spectrom.* **2003**, *9*, 305.
(27) Trikoupis, M. A.; Gerbaux, P.; Lavorato, D. J.; Flammang, R.; Terlouw, J. K. *Int. J. Mass Spectrom.* **2002**, *217*, 1.
(28) Gerbaux, P.; Barbieux-Flammang, M.; Terlouw, J. K.; Flammang, R. *Int. J. Mass Spectrom.* **2001**, *206*, 91.
(29) Heinrich, N.; Schwarz, H. In *Ion and Cluster Ion Spectroscopy and Structure*; Maier, J. P., Ed.; Elsevier: Amsterdam, 1989, p 329.
(30) Burgers, P. C.; Terlouw, J. K. In *Specialist Periodical Reports: Mass Spectrometry*; Rose, M. E., Ed.; The Royal Society of Chemistry: London, 1989; Volume 10, Chapter 2.
(31) Radom, L. *Org. Mass Spectrom.* **1991**, *26*, 359.
(32) Uggerud, E. *Mass Spectrom. Rev.* **1992**, *11*, 389.
(33) Longevialle, P. *Mass Spectrom. Rev.* **1992**, *11*, 157.
(34) Morton, T. H. *Org. Mass Spectrom.* **1992**, *27*, 353.
(35) Bowen, R. D. *Org. Mass Spectrom.* **1993**, *28*, 1577.
(36) a. Hrusak, J.; McGibbon, G. A.; Schwarz, H.; Terlouw, J. K. *Int. J. Mass Spectrom.* **1997**, *160*, 117.
(37) Troude, V.; van der Rest, G.; Mourgues, P.; Audier, H. E. *J. Am. Chem. Soc.* **1997**, *119*, 9287.
(38) Tu, Y. P.; Holmes, J. L. *J. Am. Chem. Soc.* **2000**, *122*, 3695.
(39) Tu, Y. P.; Holmes, J. L. *J. Am. Chem. Soc.* **2000**, *122*, 5597.
(40) Stirk, K. M.; Kentämaa, H. I. *J. Phys. Chem.* **1992**, *96*, 5272.
(41) Larson, J. W.; McMahon, T. B. *J. Am. Chem. Soc.* **1982**, *104*, 6255.
(42) Meot-Ner (Mautner), M. *J. Am. Chem. Soc.* **1984**, *106*, 1257−1264.
(43) Terlouw, J. K.; Heerma, W.; Burgers, P. C.; Holmes, J. L. *Can. J. Chem.* **1984**, *62*, 289.
(44) Postma, R.; Ruttink, P. J. A.; Duijneveldt, F. B.; Terlouw, J. K.; Holmes, J. L. *Can. J. Chem.* **1984**, *62*, 289.
(45) Fossey, J.; Mourgues, P.; Thissen, R.; Audier, H. E. *Int. J. Mass Spectrom.* **2003**, *227*, 373.
(46) Jeffrey, G. A.; Saenger, W. *Hydrogen Bonding in Biological Structures*; Springer-Verlag: Berlin, New York, 1991.
(47) Ben-Naim, A. *Hydrophobic Interactions*; Plenum: New York, 1980.
(48) Bernstein, M. P.; Elsila, J. E.; Dworkin, J. P.; Sandford, S. A.; Allamandola, L. J.; Zare, R. N. *Astrophys. J.* **2002**, *576*, 1115.
(49) Gudipati, M. S.; Allamandola, L. J. *Astrophys. J.* **2003**, *596*, L195.
(50) Ibrahim, Y.; Alshraeh, E.; Dias, K.; Meot-Ner (Mautner), M.; El-Shall, M. S. *J. Am. Chem. Soc.* **2004**, *126*, 12766.
(51) Ibrahim, Y. M.; Meot-Ner (Mautner), M.; Alsharaeh, E. H.; El-Shall, M. S.; Scheiner, S. *J. Am. Chem. Soc.* **2005**, *127*, 7053.
(52) Meot-Ner (Mautner), M. *Chem. Rev.* **2005**, *105*, 213.
(53) Rusyniak, M.; Ibrahim, Y.; Alsharaeh, E.; Meot-Ner, M.; El-Shall, M. S. *J. Phys. Chem. A* **2003**, *107*, 7656.
(54) Ibrahim, Y.; Alsharaeh, E.; Rusyniak, M.; Watson, S.; Meot-Ner, M.; El-Shall, M. S. *Chem. Phys. Lett.* **2003**, *380*, 21.
(55) Frisch, M. J.; Trucks, G. W.; Schlegel, H. B.; Scuseria, G. E.; Robb, M. A.; Cheeseman, J. R.; Montgomery, J. A., Jr.; Vreven, T.; Kudin, K. N.; Burant, J. C.; Millam, J. M.; Iyengar, S. S.; Tomasi, J.; Barone, V.; Mennucci, B.; Cossi, M.; Scalmani, G.; Rega, N.; Petersson, G. A.; Nakatsuji, H.; Hada, M.; Ehara, M.; Toyota, K.; Fukuda, R.; Hasegawa, J.; Ishida, M.; Nakajima, T.; Honda, Y.; Kitao, O.; Nakai, H.; Klene, M.; Li, X.; Knox, J. E.; Hratchian, H. P.; Cross, J. B.; Bakken, V.; Adamo, C.; Jaramillo, J.; Gomperts, R.; Stratmann, R. E.; Yazyev, O.; Austin, A. J.; Cammi, R.; Pomelli, C.; Ochterski, J. W.; Ayala, P. Y.; Morokuma, K.; Voth, G. A.; Salvador, P.; Dannenberg, J. J.; Zakrzewski, V. G.; Dapprich, S.; Daniels, A. D.; Strain, M. C.; Farkas, O.; Malick, D. K.; Rabuck, A. D.; Raghavachari, K.; Foresman, J. B.; Ortiz, J. V.; Cui, Q.; Baboul, A. G.; Clifford, S.; Cioslowski, J.; Stefanov, B. B.; Liu, G.; Liashenko, A.; Piskorz, P.; Komaromi, I.; Martin, R. L.; Fox, D. J.; Keith, T.; Al-Laham, M. A.; Peng, C. Y.; Nanayakkara, A.; Challacombe, M.; Gill, P. M. W.; Johnson, B.; Chen, W.; Wong, M. W.; Gonzalez, C.; Pople, J. A. *Gaussian 03*, revision C.02; Gaussian, Inc.: Wallingford, CT, 2004.
(56) Meot-Ner (Mautner), M.; Lias, S. G. Thermochemistry of Cluster Ions. *NIST Chemistry WebBook, NIST Standard Reference Database Number 69*; Linstrom, P. J., Mallard, W. G., Eds.; National Institute of Standards and Technology, Gaithersburg MD, 2003; http://webbook.nist.gov.
(57) Meot-Ner, M.; Deakyne, C. A. *J. Am. Chem. Soc.* **1985**, *107*, 469.
(58) Bohme, D. K. *Int. J. Mass Spectrom. Ion Processes* **1992**, *115*, 95.
(59) Petrie, S.; Freeman, C. G.; Meot-Ner (Mautner), G.; Ferguson, E. E. *J. Am. Chem. Soc.* **1990**, *112*, 7121.
(60) Audier, H. E.; Leblanc, D.; Mougues, P.; McMahon, T. B.; Hammerum, S. *J. Chem. Soc., Chem. Commun.* **1994**, 2329.
(61) Cunje, A.; Rodriquez, C. F.; Bohme, D. K.; Hopkinson, A. C. *J. Phys. Chem. A.* **1998**, *102*, 478.
(62) Hunter, E. P.; Lias, S. G. Proton Affinity Evaluation. In *NIST Chemistry WebBook, NIST Standard Reference Database Number 69*; Linstrom, P. J., Mallard, W. G., Eds.; National Institute of Standards and Technology: Gaithersburg MD, 2003; http://webbook.nist.gov.
(63) Davidson, W. R.; Sunner, J.; Kebarle, P. *J. Am. Chem. Soc.* **1979**, *101*, 1675.
(64) Meot-Ner, M.; Sieck, L. W. *J. Am. Chem. Soc.* **1983**, *105*, 2956.